JOC The Journal of Organic Chemistry

ARTICLE

pubs.acs.org/joc

Experimental and Theoretical Study of the 2-Alkoxyethylidene Rearrangement

Kimberly S. Graves,[†,§] Dasan M. Thamattoor,[*,†] and Paul R. Rablen[*,‡]

[†]Department of Chemistry, Colby College, Waterville, Maine 04901, United States

[‡]Department of Chemistry and Biochemistry, Swarthmore College, Swarthmore, Pennsylvania 19081-1397, United States

Supporting Information

ABSTRACT: The rearrangement of 2-ethoxyethylidene, generated photochemically from a nonnitrogenous precursor, leads to ethyl vinyl ether. Although this product could result, in principle, from a 1,2-hydrogen shift and/or a 1,2-ethoxy shift in the carbene, a deuterium labeling study indicates an essentially exclusive preference for hydrogen migration. The experimental results are in agreement with CCSD and W1BD calculations for the simpler 2-methoxyethylidene system that show a prohibitively large barrier for the methoxy shift and a negligible barrier for the hydride shift.

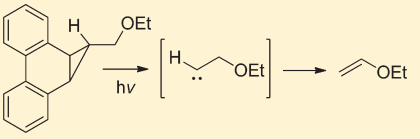

The ubiquitous 1,2-hydrogen shift is perhaps the best known reaction of many singlet carbenes bearing β-hydrogens and has attracted considerable experimental and computational scrutiny over the years.[1,2] This process, which is facilitated by the alignment of the empty p orbital on the divalent carbon with an adjacent C−H bond,[3] can be extremely rapid. For instance, the conversion of singlet methylcarbene (**1a**, X = Y = H) into ethylene (**2a**), as shown in eq 1, is too fast for experimental measurement,[4] and the barrier is estimated to be a mere 0.6[5] to 1.2[6] kcal/mol. The barrier to 1,2-hydrogen shift in **1**, however, is influenced by a number of factors including the nature of the group X at the migration terminus (C1) and Y at the migration origin (C2). When X can help stabilize the singlet carbene by hyperconjugation, as in **1b** (X = CH_3; Y = H),[7] or donation of nonbonded electrons into the vacant p orbital, e.g., **1c** (X = Cl; Y = H),[8] the rate of 1,2-hydrogen migration is substantially slowed.[9] When X is an especially powerful donor such as the methoxy group (**1d**: X = OMe; Y = H) the 1,2-hydrogen shift to produce methylvinyl ether is so severely suppressed (<10%) that it is uncompetitive with intermolecular reactions of the carbene.[10] Indeed, calculations show an excellent correlation between the σ_R values of X and the E_a for 1,2-hydrogen shift in **1**.[5]

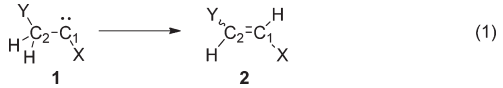

(1)

In sharp contrast, electron-donating Y groups at the migration origin *accelerate* 1,2-hydrogen shifts.[8c] For example, **1e** (X = Cl; Y = CH_3),[8e] **1f** (X = Cl; Y = Ph),[11] and **1g** ((X = Cl; Y = Cl)[12] all rearrange to the corresponding alkenes **2** at rates that are considerably faster than chloromethyl carbene **1c**. This phenomenon is referred to as "bystander assistance".[13] It has been attributed to the stabilization of the incipient positive charge on C2 by Y during the rearrangement as electron density is transferred to C1 via a transition state that resembles a hydride shift.[8c]

How well does hydrogen migrate compared to other groups? Although competition experiments seem to suggest that the inherent migratory aptitude for 1,2-shifts follows the order H > Ph > Me,[14] Nickon has proposed that such an order does not take into account the influence of bystander groups such as Y.[13] By accounting for bystander assistance, he concludes that the intrinsic migratory aptitude for these three groups actually follows the order Ph > H > Me.[13] Nickon's conclusions are supported by computational studies.[8c] Of course, reactions in excited states, especially when nitrogenous precursors such as diazirines and diazo compounds are employed, and quantum mechanical tunneling are other important considerations while analyzing the 1,2-hydrogen shift in carbenes.[1a,1b]

There are notable variations to the general theme described above, however, induced by certain heteroatom substituents at the β-position. For instance, it has been noted that the 2-norbornyl carbene **3** (R = H) prefers to undergo 1,3-C-H insertion to give **4** rather than a 1,2-hydrogen shift to produce alkene **5** as shown in eq 2.[15] The related carbene **6** (R = TMS), however, is reported to give only minor amounts of the tricyclic derivative **7** with alkene **8** now becoming the major product.[16] Most interestingly, as shown in eq 3, a labeling experiment using **9** demonstrates that both alkenes **10** (from a 1,2-hydrogen shift) and **11** (from a 1,2-TMS shift) are formed in comparable amounts (along with small amounts of the tricyclic compound **12**).[16] This remarkable result indicates that not only does the trimethylsilyl group lend "bystander" assistance to the 1,2-hydrogen shift but is also prone to migration on its own. Indeed, the thermally generated acyclic carbene **13** is reported to

Received: October 15, 2010
Published: February 22, 2011

exclusively undergo a 1,2-silyl shift to produce alkene **14** as the sole product (eq 4).[16]

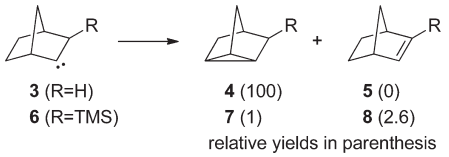

(2)

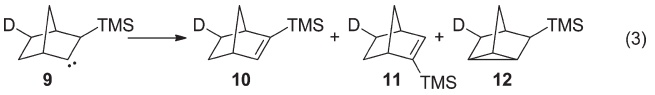

(3)

(4)

Robson and Shechter have shown that the thermal decomposition of diazo compounds **15a** and **b** lead predominantly to alkenes (**16a** and **b**), resulting from the 1,2-shift of the thio substituent and only minor amounts of **17a** and **b** from 1,2-hydrogen shift (eq 5).[17] They have attributed sulfur's penchant to undergo a 1,2-shift to its ability to interact with the divalent carbon to form a ylid type transition state **18a**. Furthermore, they suggest that alkoxy and amino substituents do not undergo analogous shifts as ylids **18b** and **c** are not available for oxygen and nitrogen respectively.

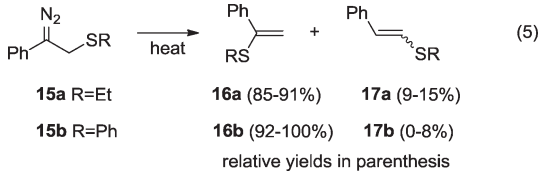

(5)

Although studies have shown that β-alkoxy groups strongly activate 1,2-hydrogen shifts in carbenes,[13,18] they do not themselves migrate to the divalent carbon.[19] A rare counter example comes from the work of Kirmse and Buschhoff, who showed that photochemical or thermal decomposition of **19** led to alkenes **20** and **21** resulting from the 1,2-shift of hydrogen and ethoxy substituent respectively in the putative carbene intermediate (eq 6).[19]

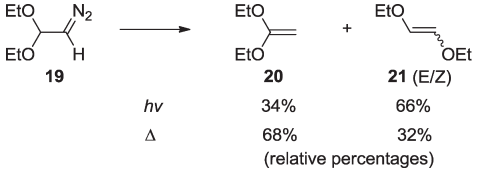

(6)

In this work we present our study of the chemistry of 2-ethoxyethylidene (**22**), a simple carbene in which a 1,2-shift of *either* the hydrogen *or* the ethoxy substituent leads to the *same* alkene, ethyl vinyl ether **23** (Scheme 1). Substituting the carbene with a deuterium, as in **24**, in principle, would lead to different isotopomers **25** (*E*/*Z*) and **26** that may be then analyzed to determine the relative importance of the two pathways. A detailed computational study is also presented.

Scheme 1. Possible Rearrangement Pathways for 2-Ethoxyethylidene and Its Deuterated Analogue

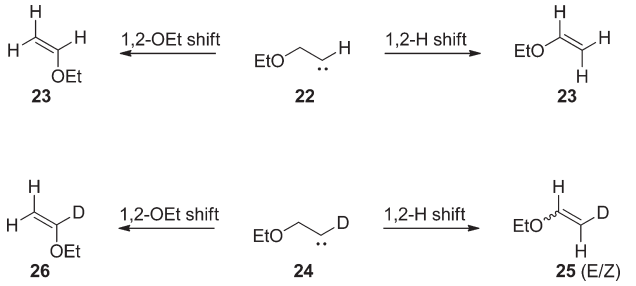

Scheme 2. Generation of Carbenes from Nitrogenous and Nonnitrogenous Sources

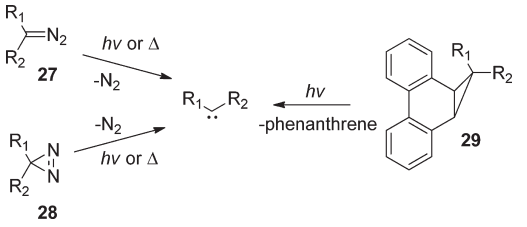

RESULTS AND DISCUSSION

Syntheses of Precursors. Although diazo compounds (**27**)[20] and diazirines (**28**)[21] have long served as the traditional sources of carbenes (Scheme 2), their use is not without complications. Considerable evidence has accumulated over the years to demonstrate that these precursors can themselves, often in their excited states, give rise to products that are identical to those issuing from real carbenes.[1,22] In particular, 1,2-hydrogen shifts to form alkenes are known to occur in the excited states of such nitrogenous sources.[4,7,23] This could lead to some confusion as to the true origin of the products. In this regard a number of groups, including ours, have employed alternative nonnitrogenous precursors such as the cyclopropanated phenanthrene system **29** as photochemical sources of carbenes.[24] In these systems, the cheletropic extrusion of carbene is accompanied by the formation of phenanthrene as a stable byproduct.

Our synthetic approach to the phenanthrene-based precursors to carbenes **22** and **24** is depicted in Scheme 3. In the first step, the hydrolysis of bromoform with aqueous base in the presence of phenanthrene (**30**) under phase transfer catalysis conditions, using our improved procedure,[25] produced the dibromocarbene adduct **31**. In the next step, **31** was treated with butyllithium at low temperatures and subsequently quenched with water to obtain the *exo*-monobromo derivative **32**.[26] Finally, the low temperature reaction of **32** with *tert*-butyllithium followed by quenching with chloromethyl ethyl ether led to **33**, the precursor

dx.doi.org/10.1021/jo1020536 |*J. Org. Chem.* 2011, 76, 1584–1591

Scheme 3. Synthesis of Nonnitrogenous Precursors to Carbenes 22 and 24

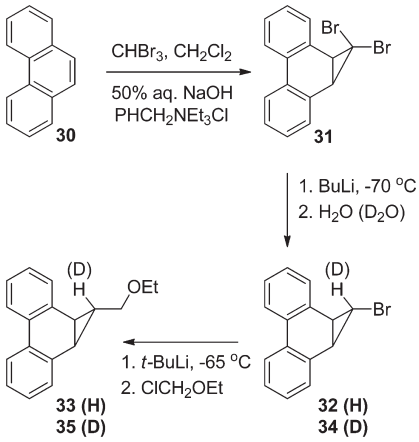

Scheme 4. Photolyses of Precursors 33 and 35

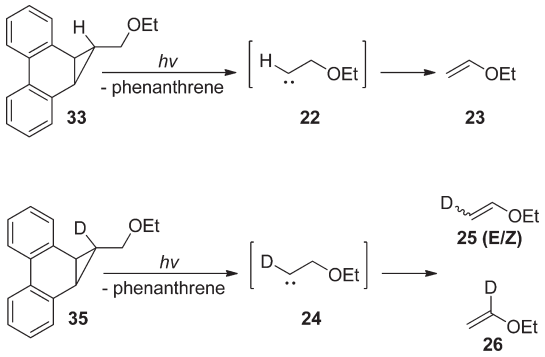

for carbene **22**. The stereochemistry of the final product was inferred from a *J* value of 4.3 Hz for the mutual coupling of the two sets of cyclopropyl protons. Density functional calculations predict 3.1 Hz for this coupling constant in the *exo* isomer but 9.2 Hz for the *endo* isomer. Furthermore, the methine hydrogen of the cyclopropyl ring is shifted somewhat upfield (δ 2.4 ppm) as it is in the shielding zone of the π system below.[24a,24b] This is typical for *trans* coupling on such ring systems.[27] Calculations confirm this interpretation, predicting a chemical shift of 2.5 ppm in the *exo* isomer but of 3.7 pm in the *endo* isomer. Quenching with D_2O instead of water in step 2 gave **34**, the deuterated version of **32**. The conversion of **34** into **35**, the precursor to carbene **24**, was accomplished by using the same final step as shown.

Photolysis Experiments. The precursor **33**, dissolved in benzene-d_6, was degassed and photolyzed in a pyrex NMR tube (or test tube) at room temperature in a Rayonet reactor. The progress of the reaction was monitored by ^{1}H NMR spectroscopy. The only product in the photolysate that was isomeric with carbene **22** was ethyl vinyl ether (**23**) (Scheme 4). A yield experiment using 1,3-benzodioxole as an internal standard revealed a maximum yield of 43% for the formation of **23**. Isolation of **23** was readily accomplished by distilling the photolysate, and its identity was confirmed by comparison to the ^{1}H and ^{13}C NMR spectra of an authentic sample obtained commercially. The photolysis of the labeled precursor **35** was carried out in a similar manner, and the labeled isotopomers of ethyl vinyl ether, **25** (*E*/*Z*) and **26**, which are isomeric with carbene **24**, also were isolated by distilling the photolysate.

The olefinic region of the ^{1}H NMR spectrum of authentic ethyl vinyl ether (**23**) is shown at the top of Figure 1. The three different types of hydrogens on the double bond are identified and integrate, as expected, to a ratio of 1:1:1. The middle spectrum in the figure shows the same region for the olefinic signals of **23** obtained from the photolysis of **33**. Once again, the three protons correctly integrate to a ratio of 1:1:1 (the peak at 4.28 ppm is an impurity). Finally, the bottom spectrum shows the olefin region of the products obtained from the photolysate of the deuterated precursor **35**. This represents the composite of the three isotopomers **25**-*E*, **25**-*Z*, and **26**. As **25**-*E* and **25**-*Z* contribute to the integral of H_a, **25**-*E* and **26** to the integral of H_b, and **25**-*Z* and **26** to the integral of H_c, the following equations can be used to relate the values of the integrals to the concentrations of the contributors.

$$\text{integral value of } H_a = I_{H_a} = [\mathbf{25}\text{-}E] + [\mathbf{25}\text{-}Z] \quad (7)$$

$$\text{integral value of } H_b = I_{H_b} = [\mathbf{25}\text{-}E] + [\mathbf{26}] \quad (8)$$

$$\text{integral value of } H_c = I_{H_c} = [\mathbf{25}\text{-}Z] + [\mathbf{26}] \quad (9)$$

The relative concentrations of the three isotopomers **25**-*E*, **25**-*Z*, and **26** may be then estimated from eqs 7, 8, and 9 as follows.

$$\frac{I_{H_a} + I_{H_b} - I_{H_c}}{2} = \frac{([\mathbf{25}\text{-}E] + [\mathbf{25}\text{-}Z]) + ([\mathbf{26}] + [\mathbf{25}\text{-}E]) - ([\mathbf{26}] + [\mathbf{25}\text{-}Z])}{2} = [\mathbf{25}\text{-}E] \quad (10)$$

$$\frac{I_{H_a} + I_{H_c} - I_{H_b}}{2} = \frac{([\mathbf{25}\text{-}E] + [\mathbf{25}\text{-}Z]) + ([\mathbf{26}] + [\mathbf{25}\text{-}Z]) - ([\mathbf{26}] + [\mathbf{25}\text{-}E])}{2} = [\mathbf{25}\text{-}Z] \quad (11)$$

$$\frac{I_{H_b} + I_{H_c} - I_{H_a}}{2} = \frac{([\mathbf{26}] + [\mathbf{25}\text{-}E]) + ([\mathbf{26}] + [\mathbf{25}\text{-}Z]) - ([\mathbf{25}\text{-}E] + [\mathbf{25}\text{-}Z])}{2} = [\mathbf{26}] \quad (12)$$

On the basis of these calculations it was determined that **25**-*E* and **25**-*Z* (in a ratio of ~1:1) made up >98% of the rearranged products with **26** comprising <2%. Thus, within the limits of experimental error, given the admittedly crude nature of these measurements, there is little doubt that there is an essentially exclusive preference for a 1,2-hydrogen shift in this system with very little, if any, 1,2-ethoxy shift.

Computational Studies. In order to shed further light on the question of hydride and alkoxy shifts in carbenes, the pathways for rearrangement of methoxyethylidene **1d** to methyl vinyl ether **2d** were also investigated via electronic structure calculations. For reasons already noted at the beginning, computational studies focused on the singlet rather than the triplet species.

dx.doi.org/10.1021/jo1020536 |*J. Org. Chem.* 2011, 76, 1584–1591

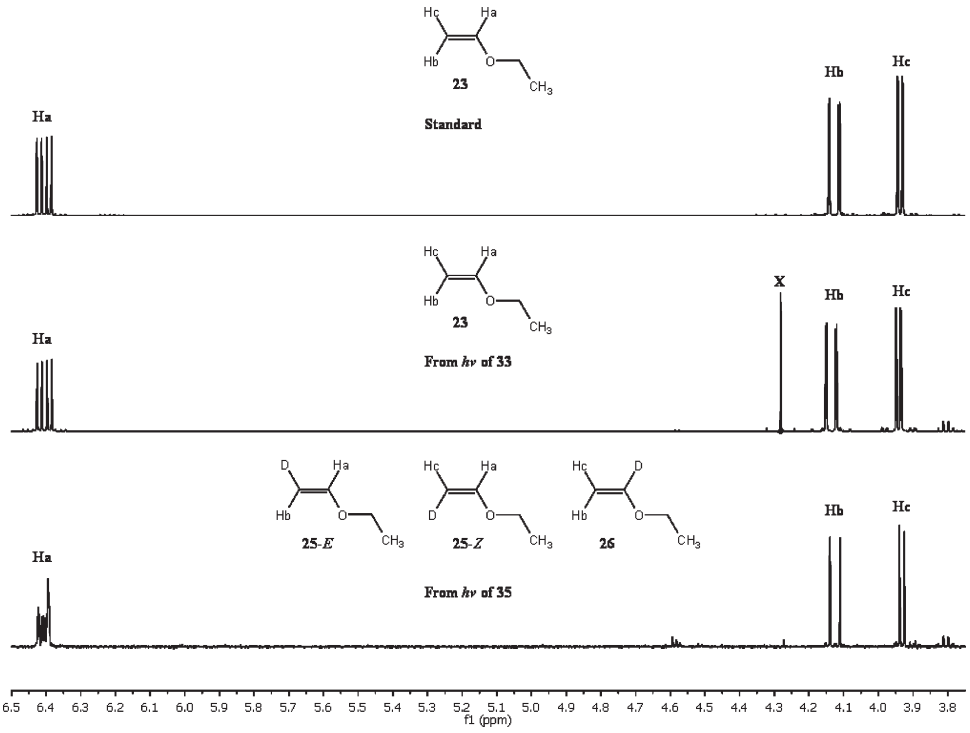

Figure 1. ^{1}H NMR spectrum of standard **23** (top), **23** from *hν* of **33** (middle), and **25** (*E*/*Z*) and **26** from *hν* of **35** (bottom).

Using the methoxy system, instead of the ethoxy system studied experimentally, considerably reduces the conformational complexity of the problem but should not qualitatively change the results. Methoxyethylidene **1d**, methyl vinyl ether **2d**, and the intermediates and transition states for hydride and methoxy shifts leading from **1d** to **2d** were subjected to calculation at several levels of theory, including G3-CCSD, W1BD, and W1BD-CCSD. The results reported correspond to computations in the gas phase. The essential results are summarized in Figure 2, which depicts the CCSD/6-31G(d) optimized geometries and the W1BD-CCSD energies of the relevant species; further details are provided in the Computational Methods section, and complete numerical results appear in the Supporting Information. As Figure 2 illustrates, the methoxy shift can occur via two diastereomeric pathways that differ slightly in energy. The same is true of the hydride shift. The methoxy pathways take place via two isomeric ylid-type intermediates (**38a** and **38b**), of the type suggested by Robson and Shechter,[17] that lie 4−8 kcal/mol above the reactant, whereas the hydride pathways lack intermediates.

In general terms, the outcome is quite unambiguous. The methoxy shift must proceed over a rather high barrier of 21 kcal/mol (transition state **39a** or **39b**). The hydride shift, on the other hand, proceeds with essentially no barrier at all. While transition states **36a** and **36b** do exist on the CCSD/6-31G(d) potential energy surface, they actually lie below the reactant after inclusion of the zero-point vibrational energy and at the W1BD level of theory. This simply means that the barrier to hydrogen migration is either nonexistent or very small whereas the barrier for the methoxy shift is quite substantial. The calculations thus unambiguously predict that the rearrangement of alkoxyethylidenes will proceed exclusively via the hydride shift and not the alkoxy shift.

Why is it so much harder for methoxide to migrate than hydride, despite the fact that one might expect a lone pair on oxygen to aid the migration process by allowing incipient formation of a new O−C bond before the old O−C bond breaks? The fact that a C−C−O bond angle is stiffer than a C−C−H bond angle perhaps plays a role.[28] Another likely factor concerns conformation. The lowest energy conformations of **1d** position two hydrogen atoms out of the plane, where they need to be located in order to initiate migration (see structure of **1d** in Figure 2). For the methoxy group to migrate, on the other hand, it is necessary for some rotation to take place about the C−C−O-C dihedral angle. Loss of whatever factors stabilize the anti conformation relative to the gauche conformation therefore probably contribute to the barrier: that is, to the energies of **39a** and **39b** relative to **1d**. These factors surely include substantial hyperconjugation of the carbene lone pair with the C−O antibonding orbital.[29]

Scheme 5 illustrates another factor that might inhibit methoxy migration. One might hypothesize that charge density redistributes itself as suggested in Scheme 5 in the transition structures for rearrangement, relative to the reactant carbene. That is, one might suppose that the migration origin loses electron density as either hydride or alkoxide migrates away from it, and gains some degree of carbocation character. Indeed, calculated atomic charges confirm that this carbon becomes 0.05−0.11 au less negative on going from reactant to either of the hydride migration transition structures and 0.12−0.22 au less negative on going from reactant to either of the methoxy migration transition structures.[30] There is consequently an important benefit to leaving behind any substituent R_1 that is a π-donor. If the hydride migrates, the electron-deficient carbon enjoys strong stabilization by the remaining methoxy group. On the other hand, if the methoxy group migrates, the remaining fragment lacks such stabilization. Indeed, the bond from the carbon that is formally positive in Scheme 5 to the methoxy oxygen shortens by 0.01−0.03 Å upon going from reactant carbene to the two possible hydride migration transition structures, suggestive of a stabilizing interaction.

dx.doi.org/10.1021/jo1020536 |*J. Org. Chem.* 2011, 76, 1584–1591

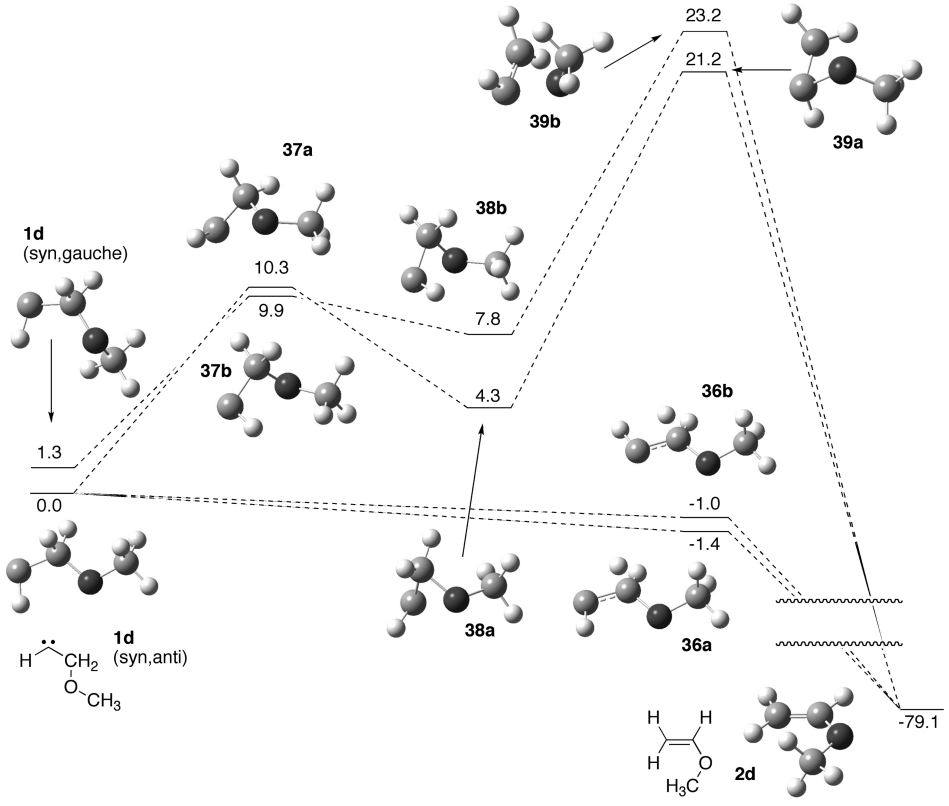

Figure 2. Rearrangement of methoxyethylidene to methyl vinyl ether via two hydride migration and two methoxy migration pathways. The structures shown were obtained by geometry optimization at CCSD/6-31G(d), and the relative energies listed, in kcal/mol, were calculated at W1BD-CCSD.

Scheme 5. Relative Stabilization of Transition States from H or OCH_3 Migration

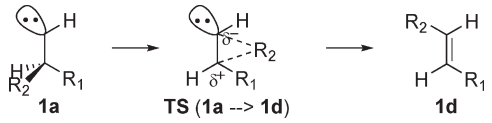

H-shift: $R_1 = OCH_3$, $R_2 = H$ (**36a**,**36b**)
CH_3O-shift: $R_1 = H$, $R_2 = OCH_3$ (**39a**,**39b**)

Scheme 6. H versus F Migration in Fluorinated Ethylidenes

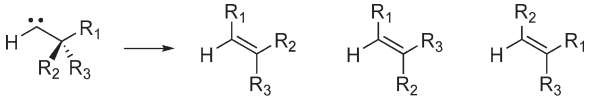

a: $R_1 = F$; $R_2 = R_3 = H$
b: $R_1 = R_3 = F$; $R_2 = H$
c: $R_1 = R_2 = R_3 = F$

If this analysis has any validity, one would predict that additional methoxy groups would at least partially equalize the playing field. If two methoxy groups were present at the migration origin, at least one would remain behind to provide stabilization regardless of which substituent migrated. This perhaps explains the experimental observation of the alkoxy group shift leading to **21**, as noted above in eq 6.[19] Similar logic would apply to the fluorinated ethylidenes in Scheme 6, which are conformationally rather simpler and therefore more amenable to computational investigation. One would expect successive fluorine substitution at the migration origin in **1a** to (a) reduce the barriers for both hydride and fluoride migration and (b) reduce the preference for hydride migration over fluoride migration. The results of exploring this idea by computational means are shown in Table 1. Indeed, the expected pattern does appear, although it is not pronounced. The barriers to hydride migration are very small to begin with, but nonetheless decrease from 0.3 to −1.5 to −2.0 kcal/mol upon substitution of first one and then a second fluorine (**1a** to **40a** to **40b**). The fluorine migration barrier, on the other hand, decreases from 33.3 kcal/mol in 2-fluoroethylidene (**40a**) to 18.8 kcal/mol in 2,2-difluoroethylidene (**40b**) and 17.7 kcal/mol in 2,2,2-trifluoroethylidene

Table 1. W1BD-CCSD Calculated Barrier Heights for the Rearrangement of Methylcarbene and Its Selected Derivatives (ΔH (0 K), kcal/mol)

reaction	barrier
1a → **2a** (H-shift)	0.3
1d → **2d** (H-shift: TS **36a**)	−1.4
1d → **2d** (O-shift: TS **39a**)	21.2
40a → **41a** (H-shift)	−1.5
40a → **41a** (F-shift)	33.3
40b → **43b** (H-shift)	−2.0
40b → **41b** (F-shift, *trans*)	18.8
40b → **42b** (F-shift, *cis*)	22.2
40c → **41c** (F-shift)	17.7

dx.doi.org/10.1021/jo1020536 |*J. Org. Chem.* 2011, 76, 1584–1591

Scheme 7. Concerted Mechanism for the Formation of Product 23 from Precursor 33

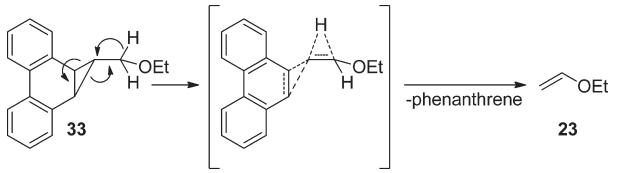

(**40c**). The calculations thus support at least to some degree the analysis put forth in Scheme 5 to help account for the high barrier to migration by the methoxy group and the very low barrier to migration by hydride.

Although the foregoing computational results and the experimentally observed preference for a 1,2-hydride shift in **22**, compared to the 1,2-ethoxy shift, are both consistent with the stepwise mechanism depicted in Figure 2, other interpretations are possible. For example, it has been suggested[31] that the calculated barrier to the hydride shift in **22** is so low that the barrier might in practice not exist at all, implying a mechanism in which the extrusion of the carbene from **33** (or **35**) and the hydride migration are concerted, leading directly to the observed product **23** (or **25**). Such a process, exemplified in Scheme 7, deserves further investigation as it raises legitimate questions about whether precursors such as **33** and **35** do in fact produce free carbenes or suffer from problems analogous to those already discussed above for nitrogenous sources.[1,22] What seems indisputable, however, is that hydride migration is greatly preferred to alkoxy migration, regardless of whether the migration and the formation of the carbene are distinct mechanistic steps or not.

CONCLUSIONS

The rearrangement of 2-ethoxyethylidene (**22**), generated from a nonnitrogenous precursor, produces ethyl vinyl ether (**23**). This product could be formed either by a 1,2-hydrogen shift or a 1,2-ethoxy shift in the carbene. By replacing the hydrogen on the carbene with a deuterium, the two pathways can be distinguished, and results indicate a virtually exclusive preference for the 1,2-hydrogen shift in the labeled carbene **24**. Electronic structure calculations confirm this conclusion, revealing little if any barrier to a hydride shift, but a barrier of more than 20 kcal/mol for an alkoxy shift. Alternatively, it is conceivable that hydride migration and carbene extrusion might be concerted.

EXPERIMENTAL AND COMPUTATIONAL METHODS

General Experimental Procedures. Tetrahydrofuran was dried by passage through two columns (2 ft × 4 in.) of activated alumina. All other solvents and reagents were used as obtained from commercial sources. All reactions were carried out under an argon atmosphere in oven-dried glassware. Column chromatography was performed on silica gel (70−230 mesh). NMR spectra were recorded at 500 MHz for ^{1}H and 125 MHz for ^{13}C in the indicated solvents. The shifts are reported in δ ppm and referenced to either tetramethylsilane (TMS) or the residual proton signal from the solvent.

***exo*-1-Bromo-1-deutero-1a,9b-dihydro-1*H*-cycpropa[*l*]phenanthrene (34).** Butyllithium (18 mL, 1.6 M in hexanes, 29 mmol) was added dropwise by syringe to a magnetically stirred solution of 1,1-dibromo-1a,9b-dihydrocycpropa[*l*]phenanthrene[25] (**31**, 9.9 g, 28 mmol) in anhydrous THF (100 mL) at −70 °C. Stirring was continued at this temperature for another 15 min after completion of addition, and the dark green reaction mixture was treated with D_2O (8 mL). The reaction mixture was then allowed to slowly warm to room temperature, and water (50 mL) was added. The organic and aqueous layers were separated, and the latter was extracted with dichloromethane (2 × 40 mL). The organic layers were combined, washed with water (2 × 40 mL) and brine (1 × 40 mL), dried over ahydrous magnesium sulfate, filtered, and freed of solvent. The crude material was purified by flash chromatography on silica gel (2 to 5% ethyl acetate in hexanes) to obtain **34** which was subsequently recrystallized from hexanes. Yield: 42%; mp 114−116 °C; ^{1}H NMR (500 MHz, $CDCl_3$) δ 7.95−7.92 (m, 2H), 7.50−7.47 (m, 2H), 7.32−7.26 (m, 4H), 3.00 (s, 2H); ^{13}C NMR (125 MHz, $CDCl_3$) δ 131.9, 129.7, 129.3, 128.1, 127.2, 123.3, 29.7; FTIR (ATR) ν 3065, 3031, 1487, 1445, 1021, 880 cm^{-1}; LRMS (EI) m/z 273 ($M^+ + 2$), 271 (M^+), 192. Anal. Calcd for $C_{18}H_{10}DBr$: C, 66.20; H, 4.44. Found: C, 66.42; H, 4.09.

***exo*-1-Bromo-1a,9b-dihydro-1*H*-cycpropa[*l*]phenanthrene (32).[26]** This was prepared as described above for **34** except that water was used instead of D_2O. Yield: 41%; mp 116−117 °C (lit.[26] 111−112 °C); ^{1}H NMR (500 MHz, $CDCl_3$) δ 7.95−7.93 (m, 2H), 7.50−7.47 (m, 2H), 7.32−7.26 (m, 4H), 3.01 (d, J = 3.2 Hz, 2H), 2.41 (t, J = 3.2 Hz, 1H); ^{13}C NMR (125 MHz, $CDCl_3$) δ 131.9, 129.7, 129.3, 128.1, 127.2, 123.3, 29.9, 27.7; FTIR (ATR) ν 3069, 3032, 1485, 1445, 1195, 978 cm^{-1}; LRMS (EI) m/z 272 ($M^+ + 2$), 270 (M^+), 191.

***exo*-1-Deutero-1-(ethoxymethyl)-1a,9b-dihydro-1*H*-cycpropa[*l*]phenanthrene (35).** A solution of *tert*-butyllithium (12 mL, 1.5 M in hexanes, 18 mmol) was added dropwise by syringe to a magnetically stirred solution of **34** (2.1 g, 7.7 mmol) in anhydrous THF (70 mL) at −65 °C. Stirring was continued at this temperature for another 1 h after completion of addition, and the dark green reaction mixture was treated with chloromethyl ethyl ether (2 mL, 21.4 mmol). Stirring was continued for 1 h at −65 °C after which the reaction mixture was allowed to slowly warm to room temperature and water (40 mL) was added. The organic and aqueous layers were separated, and the latter was extracted with dichloromethane (2 × 40 mL). The organic layers were combined, washed with water (2 × 40 mL), dried over ahydrous magnesium sulfate, filtered, and freed of solvent. The crude material was purified by flash chromatography on silica gel (2 to 5% ethyl acetate in hexanes) to obtain **35** which was subsequently recrystallized from pentane. Yield: 32%; mp 57−59 °C; ^{1}H NMR (500 MHz, $CDCl_3$) δ 7.96−7.93 (m, 2H), 7.42−7.40 (m, 2H), 7.26−7.21 (m, 4H), 3.61 (s, 2H), 3.53 (q, J = 7.0 Hz, 2H), 2.47 (s, 2H), 1.21 (t, J = 7.0 Hz, 3H); ^{13}C NMR (125 MHz, $CDCl_3$) δ 135.1, 129.4, 129.0, 127.7, 126.1, 123.1, 72.7, 65.7, 24.8, 15.3; FTIR (ATR) ν 3065, 3021, 2973, 2858, 1488, 1450, 1373, 1347, 1106, 1023 cm^{-1}; LRMS (EI) m/z 251 (M^+), 205, 192, 178. Anal. Calcd for $C_{18}H_{17}DO$: C, 86.02; H, 7.62. Found: C, 86.03; H, 7.43.

***exo*-1-(Ethoxymethyl)-1a,9b-1*H*-dihydrocycpropa[*l*]phenanthrene (33).** This was prepared starting from **32** as described above for **35**. Yield: 26%; mp 58−60 °C; ^{1}H NMR (500 MHz, C_6D_6) δ 7.83 (dd, J = 5.8, 3.4 Hz, 2H), 7.33−7.28 (m, 2H), 7.13−7.08 (m, 4H), 3.30 (d, J = 6.2 Hz, 2H), 3.24 (q, J = 7.0 Hz, 2H), 2.30 (d, J = 4.3 Hz, 2H), 1.08 (t, J = 7.0 Hz, 3H), 0.53−0.44 (m, 1H); ^{13}C NMR (125 MHz, C_6D_6) δ 134.4, 128.6, 128.0, 126.5, 125.0, 122.2, 71.1, 64.4, 24.3, 23.7, 14.1; FTIR (ATR) ν 3066, 3021, 2973, 2859, 1488, 1451, 1373, 1348, 1105, 952 cm^{-1}; LRMS (EI) m/z 250 (M^+), 204, 191, 178. Anal. Calcd for $C_{18}H_{18}O$: C, 86.36; H, 7.25. Found: C, 85.94; H, 7.47.

General Procedure for Photolysis. In a typical experiment the precursor was dissolved in benzene-d_6, degassed, and photolyzed in a pyrex NMR tube (or test tube) using a Rayonet photochemical reactor. The progress of the reaction was monitored by NMR, and the starting material was consumed in about 20−24 h. The photolysate was distilled under vacuum to isolate volatile products, and the distillate was analyzed by NMR. The yield experiment was carried out in an analogous manner except that a precisely weighed amount of 1,3-benzodioxole was used as an internal standard.

dx.doi.org/10.1021/jo1020536 |*J. Org. Chem.* 2011, 76, 1584–1591

Computational Methods. In order to predict NMR properties of the *exo* and *endo* isomers of **32**, the geometries of the two structures were first optimized at B3LYP/6-31G(d). Isotropic magnetic shielding values (chemical shifts) were then computed via single point calculations, using the GIAO method,[32] Cramer's WP04 functional designed for computing proton chemical shifts,[33] the 6-31G(d,p) basis set, a simulated chloroform solvent (Polarizable Continuum Model, scrf=chloroform),[34] and the empirical scaling parameters reported by Jain, Bally, and Rablen.[35] Coupling constants were computed using a B3LYP/6-31G(d,p) single point calculation, the NMR=spinspin keyword,[36] and the method developed by Deng, Cheeseman, and Frisch for augmenting and uncontracting the core portion of the basis set when computing the Fermi contact term (invoked using the "mixed" option in Gaussian).[37]

Structures and energies relevant to the hydride and methoxide shift pathways for rearrangement of carbene **1d** to methyl vinyl ether **2d** were computed at HF/6-31G(d), B3LYP/cc-pVTZ+d, and CCSD/6-31G(d). Transition structures were located either via an initial partial optimization with one or two internal coordinates frozen, yielding a structure close enough to the transition structure for a full optimization to converge, or through use of Schlegel's quasi-Newton synchronous transit methods (QST2 and QST3).[38] Frequency calculations were carried out at all three levels of theory in order to confirm the nature of each stationary point. The identity of each transition state was confirmed by intrinsic reaction coordinate (IRC) following at CCSD/6-31G(d). The end point structures from the IRC calculations were further optimized without constraint to confirm that the transition structures indeed linked the minima indicated in Figure 2. T1 diagnostic values were calculated and were in a reasonable range (most below 0.02, all below 0.04).

In order to obtain more reliable energies, three higher-level procedures were performed. The CCSD/6-31G(d) geometries were used as the basis of G3-CCSD and W1BD-CCSD calculations, denoting, respectively, G3[39] and W1BD[40] calculations in which CCSD/6-31G(d) geometry optimization and frequency calculations replace the optimization and frequency calculations ordinarily prescribed by these recipes. This approach has been used previously to good effect in carbene reactions.[41] Regular W1BD calculations, which use B3LYP/cc-pVTZ+d optimization and frequency calculation, were carried out as well, although some minima and transition states did not exist on the potential energy surface at this level of theory. In all cases, the energies reported correspond to electronic energies with a zero-point vibrational energy correction, i.e., enthalpies at 0 K. Atomic charges were derived using Weinhold's NPA procedure[42] carried out with B3LYP/aug-cc-pVTZ single-point calculations performed at the CCSD/6-31G(d) geometries.

All calculations were performed using the Gaussian 09[43] and Gaussian 03[44] packages.

■ ASSOCIATED CONTENT

Supporting Information. Copies of ^{1}H and ^{13}C NMR spectra, FTIR spectra, and GC/MS data for **32**, **33**, **34**, and **35**. Table of calculated energies and NMR properties of **32** (*exo* and *endo* isomers). Tables of calculated energies, T1 diagnostic values, key atomic charges, and key bond distances and angles of structures involved in the hydride and alkoxy shifts of **1d** and of structures involved in the hydride and fluoride shifts in Scheme 6. Cartesian coordinates of CCSD/6-31G(d) optimized structures. This material is available free of charge via the Internet at http://pubs.acs.org.

■ AUTHOR INFORMATION

Corresponding Author

*E-mail: (D.M.T.) dmthamat@colby.edu; (P.R.R.) prablen1@swarthmore.edu

Present Addresses

[§]Department of Chemistry, Princeton University, Princeton, NJ 08544.

■ ACKNOWLEDGMENT

We gratefully acknowledge support of this work by the National Science Foundation through grant number CHE-0719335. This research was supported in part by the National Science Foundation through TeraGrid resources provided by NCSA under grant number TRA100004.

■ REFERENCES

(1) (a) Jones, M., Jr.; Moss, R. A. In *Reactive Intermediate Chemistry*; Moss, R. A., Platz, M. S., Jones, M., Jr., Eds.; Wiley-Interscience: Hoboken, NJ, 2004; p 273. (b) Merrer, D. C.; Moss, R. A. In *Advances in Carbene Chemistry*; Brinker, U. H., Ed.; Elsevier: Amsterdam, 2001; Vol. 3, p 53. (c) Bonneau, R.; Liu, M. T. H. In *Advances in Carbene Chemistry*; Brinker, U. H., Ed.; JAI Press: Stamford, CT, 1998; Vol. 2, p 1. (d) Moss, R. A. In *Advances in Carbene Chemistry*; Brinker, U. H., Ed.; JAI Press: Stamford, CT, 1994; Vol. 1, p 59.

(2) As triplet carbenes generally do not undergo 1,2-hydrogen shifts, this study is focused on the singlet species. See: Conrad, M. P.; Schaefer, H. F., III *J. Am. Chem. Soc.* **1978**, *100*, 7820 and references therein.

(3) (a) Nickon, A.; Bronfenbrenner, J. K. *J. Am. Chem. Soc.* **1982**, *104*, 2022. (b) Press, L. S.; Shechter, H. *J. Am. Chem. Soc.* **1979**, *101*, 509.

(4) Seburg, R. A.; McMahon, R. J. *J. Am. Chem. Soc.* **1992**, *114*, 7183.

(5) Evanseck, J. D.; Houk, K. N. *J. Phys. Chem.* **1990**, *94*, 5518.

(6) (a) Ma, B.; Schaefer, H. F., III *J. Am. Chem. Soc.* **1994**, *116*, 3539. (b) Miller, D. M.; Schreiner, P. R.; Schaefer, H. F., III *J. Am. Chem. Soc.* **1995**, *117*, 4137.

(7) Modarelli, D. A.; Morgan, S.; Platz, M. S. *J. Am. Chem. Soc.* **1992**, *114*, 7034.

(8) (a) Albu, T. V.; Lynch, B. J.; Truhlar, D. G.; Goren, A. C.; Hrovat, D. A.; Borden, W. T.; Moss, R. A. *J. Phys. Chem. A* **2002**, *106*, 5323. (b) Kraka, E.; Cremer, D. *J. Phys. Org. Chem.* **2002**, *15*, 431. (c) Keating, A. E.; Garcia-Garibay, M. A.; Houk, K. N. *J. Phys. Chem. A* **1998**, *102*, 8467. (d) Dix, E. J.; Herman, M. S.; Goodman, J. L. *J. Am. Chem. Soc.* **1993**, *115*, 10424. (e) LaVilla, J. A.; Goodman, J. L. *J. Am. Chem. Soc.* **1989**, *111*, 6877. (f) Liu, M. T. H.; Bonneau, R. *J. Am. Chem. Soc.* **1989**, *111*, 6873.

(9) Hill, B. T.; Zhu, Z.; Boeder, A.; Hadad, C. M.; Platz, M. S. *J. Phys. Chem. A* **2002**, *106*, 4970.

(10) Sheridan, R. S.; Moss, R. A.; Wilk, B. K.; Shen, S.; Wlostowski, M.; Kesselmayer, M. A.; Subramanian, R.; Kmiecik-Lawrynowicz, G.; Krogh-Jespersen, K. *J. Am. Chem. Soc.* **1988**, *110*, 7563.

(11) Liu, M. T. H.; Bonneau, R. *J. Am. Chem. Soc.* **1990**, *112*, 3915.

(12) Bonneau, R.; Liu, M. T. H.; Kim, K. C.; Goodman, J. L. *J. Am. Chem. Soc.* **1996**, *118*, 3829.

(13) Nickon, A. *Acc. Chem. Res.* **1993**, *26*, 84.

(14) (a) Pomerantz, M.; Witherup, T. H. *J. Am. Chem. Soc.* **1973**, *95*, 5977. (b) Sargeant, P. B.; Shechter, H. *Tetrahedron Lett.* **1964**, 3957. (c) Philip, H.; Keating, J. *Tetrahedron Lett.* **1961**, 523.

(15) (a) Friedman, L.; Shechter, H. *J. Am. Chem. Soc.* **1961**, *83*, 3159. (b) Freeman, P. K.; George, D. E.; Rao, V. N. M. *J. Org. Chem.* **1964**, *29*, 1682.

(16) Creary, X.; Wang, Y. X. *Tetrahedron Lett.* **1989**, *30*, 2493.

(17) Robson, J. H.; Shechter, H. *J. Am. Chem. Soc.* **1967**, *89*, 7112.

(18) Olmstead, K. K.; Nickon, A. *Tetrahedron* **1998**, *54*, 12161.

(19) Kirmse, W.; Buschhoff, M. *Chem. Ber.* **1967**, *100*, 1491.

(20) (a) Zollinger, H. *Diazo Chemistry II*; VCH: Weinheim, 1995. (b) Regitz, M.; Maas, G. *Diazo Compounds: Properties and Synthesis*; Academic Press: Orlando, 1986.

(21) (a) Moss, R. A. *Acc. Chem. Res.* **2006**, *39*, 267.(b) *Chemistry of Diazirines*; Liu, M. T. H., Ed.; CRC Press: Boca Raton, 1987; Vols. I and II.

(22) Platz, M. S. In *Advances in Carbene Chemistry*; Brinker, U. H., Ed.; JAI Press: Stamford, CT, 1998; Vol. 2, p 133.

(23) (a) Zhang, Y.; Kubicki, J.; Platz, M. S. *Org. Lett.* **2010**, *12*, 3182. (b) Burdzinski, G.; Zhang, Y.; Selvaraj, P.; Sliwa, M.; Platz, M. S. *J. Am. Chem. Soc.* **2010**, *132*, 2126. (c) Wang, J.; Burdzinski, G.; Gustafson, T. L.; Platz, M. S. *J. Am. Chem. Soc.* **2007**, *129*, 2597. (d) Motschiedler, K.; Gudmundsdottir, A.; Toscano, J. P.; Platz, M.; Garcia-Garibay, M. A. *J. Org. Chem.* **1999**, *64*, 5139. (e) Ford, F.; Yuzawa, T.; Platz, M. S.; Matzinger, S.; Fuelscher, M. *J. Am. Chem. Soc.* **1998**, *120*, 4430. (f) Celebi, S.; Leyva, S.; Modarelli, D. A.; Platz, M. S. *J. Am. Chem. Soc.* **1993**, *115*, 8613. (g) White, W. R., III; Platz, M. S. *J. Org. Chem.* **1992**, *57*, 2841.

(24) (a) Farlow, R. A.; Thamattoor, D. M.; Sunoj, R. B.; Hadad, C. M. *J. Org. Chem.* **2002**, *67*, 3257. (b) Thamattoor, D. M.; Snoonian, J. R.; Sulzbach, H. M.; Hadad, C. M. *J. Org. Chem.* **1999**, *64*, 5886. (c) Nigam, M.; Platz, M. S.; Showalter, B. M.; Toscano, J. P.; Johnson, R.; Abbot, S. C.; Kirchhoff, M. M. *J. Am. Chem. Soc.* **1998**, *120*, 8055. (d) Robert, M.; Likhotvorik, I.; Platz, M. S.; Abbot, S. C.; Kirchoff, M. M.; Johnson, R. *J. Phys. Chem. A* **1998**, *102*, 1507. (e) Ruck, R. T.; Jones, M., Jr. *Tetrahedron Lett.* **1998**, *39*, 2277. (f) Ruck, R. T.; Jones, M., Jr. *Tetrahedron Lett.* **1998**, *39*, 4433. (g) Glick, H. C.; Likhovorik, I. R.; Jones, M., Jr. *Tetrahedron Lett.* **1995**, *36*, 5715. (h) Chateauneuf, J. E.; Johnson, R. P.; Kirchhoff, M. M. *J. Am. Chem. Soc.* **1990**, *112*, 3217. (i) Richardson, D. B.; Durrett, L. R.; Martin, J. M., Jr.; Putnam, W. E.; Slaymaker, S. C.; Dvoretzky, I. *J. Am. Chem. Soc.* **1965**, *87*, 2763.

(25) Nguyen, J. M.; Thamattoor, D. M. *Synthesis* **2007**, 2093.

(26) (a) Schaeffler, J.; Deppisch, B.; Retey, J. *Chem. Ber.* **1982**, *115*, 2229. (b) Schaeffler, J.; Retey, J. *Angew. Chem.* **1978**, *90*, 906.

(27) Wan, P.; Budac, D.; Earle, M.; Shukla, D. *J. Am. Chem. Soc.* **1990**, *112*, 8048.

(28) One can estimate the force constant for bending the HCC bond angle by carrying out successive B3LYP/6-31G(d) partial optimizations on ethanol, in which CS symmetry is maintained, and all geometric parameters except the HCC bond angle are allowed to vary, but the HCC angle for the H atom *anti* to the oxygen is forcibly compressed in 2° increments until 30° of distortion is achieved. Fitting to a simple parabola (Hooke's Law) then yields a force constant of 0.0179 hartree/deg.^{2} An analogous procedure yields a force constant of 0.0363 hartree/deg^2 for compressing the OCC bond angle. Using this approach thus yields a ratio of 2.02 for the bending force constants of OCC and HCC bond angles.

(29) For instance, when the methoxy group goes from a *syn* to an *anti* orientation with respect to the carbene lone pair, the CC−OC bond length increases from 1.409 to 1.418 Å. Similarly, a natural bond orbital (NBO) analysis shows that the donation from the carbon (carbene) lone pair into the C-O antibonding orbital increases from 4.2 to 10.5 kcal/mol (B3LYP/aug-cc-pVTZ//CCSD/6-31G(d) NBO analysis).

(30) The atomic charges were computed at B3LYP/aug-cc-pVTZ//CCSD/6-31G(d), using Weinhold's NPA procedure. While the carbon in question does become less negative, as expected from the resonance structure in Scheme 5, the migrating group does not become more negative. Instead, it is the other carbon atom that increases in negative charge.

(31) We thank our associate editor, Professor Daniel Singleton, for alerting us to this possibility during the review process.

(32) (a) Cheeseman, J. R.; Trucks, G. W.; Keith, T. A.; Frisch, M. J. *J. Chem. Phys.* **1996**, *104*, 5497. (b) Wolinski, K.; Hinton, J. F.; Pulay, P. *J. Am. Chem. Soc.* **1990**, *112*, 8251. (c) Ditchfield, R. *Mol. Phys.* **1974**, *27*, 789.

(33) Wiitala, K. W.; Hoye, T. R.; Cramer, C. J. *J. Chem. Theory Comput.* **2006**, *2*, 1085.

(34) For a review of this and other methods of including a simulated solvent, see: Tomasi, J.; Mennucci, B.; Cammi, R. *Chem. Rev.* **2005**, *105*, 2999.

(35) Jain, R.; Bally, T.; Rablen, P. R. *J. Org. Chem.* **2009**, *74*, 4017.

(36) (a) Peralta, J. E.; Scuseria, G. E.; Cheeseman, J. R.; Frisch, M. J. *Chem. Phys. Lett.* **2003**, *375*, 452. (b) Sychrovsky, V.; Grafenstein, J.; Cremer, D. *J. Chem. Phys.* **2000**, *113*, 3530. (c) Helgaker, T.; Watson, M.; Handy, N. C. *J. Chem. Phys.* **2000**, *113*, 9402.

(37) Deng, W.; Cheeseman, J. R.; Frisch, M. J. *J. Chem. Theory Comput.* **2006**, *2*, 1028.

(38) (a) Peng, C.; Ayala, P.; Schlegel, H. B.; Frisch, M. J. *J. Comput. Chem.* **1996**, *17*, 49. (b) Peng, C.; Schlegel, H. B. *Isr. J. Chem.* **1994**, *33*, 449.

(39) Curtiss, L. A.; Raghavachari, K.; Redfern, P. C.; Rassolov, V.; Pople, J. A. *J. Chem. Phys.* **1998**, *109*, 7764.

(40) (a) Barnes, E. C.; Petersson, G. A.; Montgomery, J. A.; Frisch, M. J.; Martin, J. M. L. *J. Chem. Theory Comput.* **2009**, *5*, 2687. (b) Martin, J. M. L.; de Oliveira, G. *J. Chem. Phys.* **1999**, *111*, 1843.

(41) Rablen, P. R.; Paiz, A. A.; Thuronyi, B. W.; Jones, M., Jr. *J. Org. Chem.* **2009**, *74*, 4252.

(42) Reed, A. E.; Weinstock, R. B.; Weinhold, F. *J. Chem. Phys.* **1985**, *83*, 735.

(43) Frisch, M. J.; Trucks, G. W.; Schlegel, H. B.; Scuseria, G. E.; Robb, M. A; Cheeseman, J. R.; Scalmani, G.; Barone, V.; Mennucci, B.; Petersson, G. A.; Nakatsuji, H.; Caricato, M.; Li, X.; Hratchian, H. P.; Izmaylov, A. F.; Bloino, J.; Zheng, G.; Sonnenberg, J. L.; Hada, M.; Ehara, M.; Toyota, K.; Fukuda, R.; Hasegawa, J.; Ishida, M.; Nakajima, T.; Honda, Y.; Kitao, O.; Nakai, H.; Vreven, T.; Montgomery, J. A., Jr.; Peralta, J. E.; Ogliaro, F.; Bearpark, M.; Heyd, J. J.; Brothers, E.; Kudin, K. N.; Staroverov, V. N.; Kobayashi, R.; Normand, J.; Raghavachari, K.; Rendell, A.; Burant, J. C.; Iyengar, S. S.; Tomasi, J.; Cossi, M.; Rega, N.; Millam, J. M.; Klene, M.; Knox, J. E.; Cross, J. B.; Bakken, V.; Adamo, C.; Jaramillo, J.; Gomperts, R.; Stratmann, R. E.; Yazyev, O.; Austin, A. J.; Cammi, R.; Pomelli, C.; Ochterski, J. W.; Martin, R. L.; Morokuma, K.; Zakrzewski, V. G.; Voth, G. A.; Salvador, P.; Dannenberg, J. J.; Dapprich, S.; Daniels, A. D.; Farkas, O.; Foresman, J. B.; Ortiz, J. V.; Cioslowski, J.; Fox, D. J. *Gaussian 09, Revision A.02*; Gaussian, Inc.: Wallingford, CT, 2009.

(44) Frisch, M. J.; Trucks, G. W.; Schlegel, H. B.; Scuseria, G. E.; Robb, M. A; Cheeseman, J. R.; Montgomery, J. A., Jr.; Vrevnen, T.; Kudin, K. N.; Burant, J. C.; Millam, J. M.; Iyengar, S. S.; Tomasi, J.; Barone, V.; Mennucci, B.; Cossi, M.; Scalmani, G.; Rega, N.; Petersson, G. A.; Nakatsuji, H.; Hada, M.; Ehara, M.; Toyota, K.; Fukuda, R.; Hasegawa, J.; Ishida, M.; Nakajima, T.; Honda, Y.; Kitao, O.; Nakai, H.; Klene, M.; Li, X.; Knox, J. E.; Hratchian, H. P.; Cross, J. B.; Adamo, C.; Jaramillo, J.; Gomperts, R.; Stratmann, R. E.; Yazyev, O.; Austin, A. J.; Cammi, R.; Pomelli, C.; Ochterski, J. W.; Ayala, P. Y.; Morokuma, K.; Voth, G. A.; Salvador, P.; Dannenberg, J. J.; Zakrzewski, V. G.; Dapprich, S.; Daniels, A. D.; Strain, M. C.; Farkas, O.; Malick, D. K.; Rabuck, A. D.; Raghavachari, K.; Foresman, J. B.; Ortiz, J. V.; Cui, Q.; Baboul, A. G.; Clifford, S.; Cioslowski, J.; Stefanov, B. B.; Liu, G.; Liashenko, A.; Piskorz, P.; Komaromi, I.; Martin, R. L.; Fox, D. J.; Keith, T.; Al-Laham, M. A.; Peng, C. Y.; Nanayakkara, A.; Challacombe, M.; Gill, P. M. W.; Johnson, B.; Chen, W.; Wong, M. W.; Gonzalez, C.; Pople, J. A. *Gaussian 03, Revision C.02*; Gaussian, Inc.: Wallingford, CT, 2009.